



# Salmonella biofilms program innate immunity for persistence in *Caenorhabditis elegans*

Stuti K. Desai<sup>a</sup>, Anup Padmanabhan<sup>a,1</sup>, Sharvari Harshe<sup>a</sup>, Ronen Zaidel-Bar<sup>b</sup>, and Linda J. Kenney<sup>a,c,2</sup>

<sup>a</sup>Mechanobiology Institute, T-Lab, National University of Singapore, Singapore 117411; <sup>b</sup>Department of Cell and Developmental Biology, Sackler Faculty of Medicine, Tel Aviv University, Tel Aviv 69978, Israel; and <sup>c</sup>Department of Biochemistry and Molecular Biology, University of Texas Medical Branch, Galveston, TX 77555

Edited by E. Peter Greenberg, University of Washington, Seattle, WA, and approved May 10, 2019 (received for review December 27, 2018)

**The adaptive in vivo mechanisms underlying the switch in *Salmonella enterica* lifestyles from the infectious form to a dormant form remain unknown. We employed *Caenorhabditis elegans* as a heterologous host to understand the temporal dynamics of *Salmonella* pathogenesis and to identify its lifestyle form in vivo. We discovered that *Salmonella* exists as sessile aggregates, or in vivo biofilms, in the persistently infected *C. elegans* gut. In the absence of in vivo biofilms, *Salmonella* killed the host more rapidly by actively inhibiting innate immune pathways. Regulatory cross-talk between two major *Salmonella* pathogenicity islands, SPI-1 and SPI-2, was responsible for biofilm-induced changes in host physiology during persistent infection. Thus, biofilm formation is a survival strategy in long-term infections, as prolonging host survival is beneficial for the parasitic lifestyle.**

*Salmonella* | biofilms | carrier state | CsgD | SsrB

Intracellular survival of *Salmonella* Typhimurium requires the activation of a genetic program, which involves two distinct type III secretion systems encoded on *Salmonella* pathogenicity islands 1 and 2 (SPI-1 and SPI-2). Activation of SPI-1 catalyzes the uptake of *Salmonella* across the intestinal epithelium (reviewed in ref. 1), whereas SPI-2 genes are required for survival in an acidic vacuole (2–4). For host transmission and in vivo persistence, *Salmonella* relies on its ability to form multicellular communities (5). A hallmark of *Salmonella* carriage is the formation of biofilms on gallstones of asymptomatic patients (6), and a significant proportion of *Salmonella* carriers ultimately develop hepatobiliary carcinomas (7).

A clear understanding of *Salmonella* biofilms and their role in pathogenesis is lacking due to the absence of in vivo evidence of biofilm-driven dormancy during asymptomatic carriage. In this regard, the mouse model of infection has proven to be limited, due, in part, to the inability to determine the lifestyle features of *Salmonella*-colonized organs. In other gram-negative pathogens such as *Vibrio cholerae*, it has been established that the bacteria residing within host-associated biofilms exhibit enhanced virulence compared with those adapted to the planktonic lifestyle (8, 9). In the present work, we determine that for *Salmonella*, the biofilm lifestyle is advantageous for persistence in the host compared with the more detrimental infections caused by planktonic cells.

Activation of SPI-2 genes in *Salmonella* requires the sensor kinase SsrA and its cognate transcription factor SsrB, which, together, comprise the SsrA/B two-component regulatory system (TCRS) (2–4). In our earlier work, we identified SsrB as a novel molecular switch in *Salmonella* Typhimurium that acts to drive two distinct lifestyle fates. In the phosphorylated form, SsrB~P activates the transcription of virulence genes that promote the intravacuolar lifestyle (4, 10, 11). At neutral intracellular pH 6.8 (12), the levels of SsrA kinase are low (13), and unphosphorylated SsrB drives the formation of biofilms by up-regulating the expression of the master regulator gene *csgD* (5 and reviewed in ref. 14). An increase in CsgD levels leads to enhanced curli fiber expression, as well as up-regulation of matrix components (ref. 15 and references therein). We now harness the *Caenorhabditis elegans*

infection model (16, 17) to extend our understanding of colonization dynamics during persistent infections by *Salmonella*. In this simple model host, *Salmonella* forms biofilms in the intestinal lumen. Superresolution imaging of these static aggregates determined that they vary in area from 10 to 60  $\mu\text{m}^2$  and they express all of the hallmarks of in vitro biofilms. Surprisingly, biofilm formation activated host defenses, leading to growth advantages in vivo. During biofilm-favoring conditions, *Salmonella* SPI-1 virulence genes were down-regulated, allowing the appropriate functioning of host innate immunity pathways. In an *ssrB*-null strain, biofilms did not form, toxin genes were up-regulated, and host survival was reduced. Thus, formation of the carrier state in the form of biofilms alters host physiology to promote survival, enabling persistence of *Salmonella* in the host. This may be akin to how *Salmonella* survives in distal sites such as the gallbladder, liver, and spleen.

## Results

***Salmonella* Forms Aggregates in the *C. elegans* Intestine.** We were interested in exploring *Salmonella* lifestyle changes in vivo after infection in *C. elegans*. Toward this aim, we infected fourth-stage *C. elegans* larvae (L4) with wild-type *Salmonella* expressing mCherry and compared it with an *ssrB*-null strain. Larvae fed on the *Escherichia coli* strain OP50-mCherry served as a control. Confocal fluorescence imaging of live, persistently infected worms at 2, 4, and 6 d postinfection (dpi) clearly showed that both wild-type *Salmonella* and the *ssrB*-null mutant were able to

## Significance

*Salmonella* resides as an intracellular pathogen in eukaryotic hosts and causes diarrhea or typhoid fever. In a small but alarming proportion of infected humans, *Salmonella* exists asymptotically as biofilms, a basis for long-term disease transmission. Although *Salmonella* biofilms have been observed in chronically infected mice, mechanisms underlying why and how such multicellular aggregates are formed in vivo remain poorly understood. We exposed optically transparent *Caenorhabditis elegans* to *Salmonella* and observed the progression of infection in intestines from free-living cells to static aggregates. We discovered that a secreted toxin is down-regulated when *Salmonella* forms biofilms, leading to an adaptive advantage in chronic infections. Hence, *Salmonella* biofilms enable dormancy to prolong in vivo existence.

Author contributions: S.K.D., A.P., and L.J.K. designed research; S.K.D., A.P., and S.H. performed research; R.Z.-B. contributed new reagents/analytic tools; S.K.D., A.P., and S.H. analyzed data; and S.K.D. and L.J.K. wrote the paper.

The authors declare no conflict of interest.

This article is a PNAS Direct Submission.

Published under the PNAS license.

<sup>1</sup>Present address: Department of Biological Sciences, Ashoka University, Sonapat, Haryana 131029, India.

<sup>2</sup>To whom correspondence may be addressed. Email: likenney@utmb.edu.

This article contains supporting information online at [www.pnas.org/lookup/suppl/doi:10.1073/pnas.1822018116/-DCSupplemental](http://www.pnas.org/lookup/suppl/doi:10.1073/pnas.1822018116/-DCSupplemental).

successfully colonize worm intestines (Fig. 1A). However, there was a marked difference in the colonization characteristics of wild-type *Salmonella* at 6 dpi compared with the *ssrB*-null strain. In the wild-type infection, discrete fluorescent clusters or aggregates were visible in the intestinal lumen. In contrast, in the *ssrB*-null-infected intestines, only individual mCherry bacteria were evident at 6 dpi (Fig. 1A). No fluorescent signal was detected in the worms fed on the control OP50 strain at 2, 4, or 6 d (Fig. 1A). Unphosphorylated SsrB was sufficient to enable the formation of in vivo aggregates, as observed in worms infected with a D56A SsrB mutant (SI Appendix, Fig. S1). This result corroborated the genetic inability of the *ssrB*-null strain to form aggregates in vivo, as established in our previous studies in vitro (5). The inability of the *ssrB* mutant to exist as intestinal aggregates in vivo was not due to mere growth differences, as *Salmonella* counts recovered from *ssrB*-infected worms were not significantly different from the wild-type infections at 6 dpi (SI Appendix, Fig. S2).

A closer examination also revealed differences in gut distension as a result of persistent infections by wild-type and *ssrB*-mutant *Salmonella* strains. The lumen of worms infected with either a wild-type or *ssrB*-null strain showed increased distension compared with the control *E. coli*-fed worms (Fig. 1A and B). This distension resulted in a pathogen-driven constipation phenotype (17, 18). Surprisingly, in the *ssrB* mutant, the intestinal lumen width at 6 dpi was nearly twice as distended as the lumen

of worms infected with wild-type *Salmonella* ( $\sim 14 \mu\text{m}$  compared with  $\sim 7 \mu\text{m}$ ), indicating a stronger response to the infection (Fig. 1A and B). Finally, we obtained a higher resolution view of the spatial characteristics of wild-type aggregates at 6 dpi by super-resolution imaging and confirmed their presence in the intestinal lumen (Fig. 1C and Movie S1).

**Salmonella Aggregates Are Static and Vary in Size.** When bacteria switch to a sedentary lifestyle, they come together to form aggregates that ultimately develop to form mature biofilms that can lead to persistent infections (19). In *Salmonella* Typhimurium, this lifestyle switch requires transcriptional activation of the central biofilm regulator, CsgD, by the atypical response regulator, SsrB (reviewed in ref. 14). To understand the nature of the *Salmonella* aggregates in the intestinal lumen at 6 dpi, we compared wild-type aggregates with the individual fluorescent bacteria in the *ssrB*-null infections (Fig. 1A). Time-lapse recordings revealed that the aggregates in the intestines of wild-type-infected worms remained static for the duration of a 300-s recording (Fig. 2A and Movie S2). In contrast, the fluorescent molecules visualized in the *ssrB*-null infections were mobile throughout the entire intestine (Fig. 2A and Movie S3). These findings established that wild-type *Salmonella* formed static, SsrB-dependent aggregates in vivo. Determination of the aggregate area formed by the wild-type *Salmonella* strain indicated a range from  $10\text{--}60 \mu\text{m}^2$  (Fig. 2B and C). However, in the *ssrB*-null-infected worms, most aggregates were  $<10 \mu\text{m}^2$ , with 90% of the aggregates in the range of  $2\text{--}7 \mu\text{m}^2$  (Fig. 2D). Thus, we established that wild-type *Salmonella* aggregates were static and ranged in size from  $10\text{--}60 \mu\text{m}^2$ , and that their formation required SsrB.

**Salmonella Aggregates Express Biofilm Markers.** We next investigated whether the static SsrB-dependent aggregates formed by wild-type *Salmonella* were in vivo biofilms. Biofilms require expression of the master regulator of biofilms, CsgD, and the quintessential biofilm matrix components, curli fibers (composed of CsgA monomers) and cellulose (20–22). Interestingly, the aggregative phenotype was also lost in the intestines of worms fed with the *csgD csgA* double mutant, indicating a requirement for *Salmonella* biofilm components (SI Appendix, Fig. S3). Immunofluorescence analysis of isolated intestines using anti-CsgD, anti-CsgA, and anti-O-antigen antibodies detected the presence of CsgD and CsgA (Fig. 3A) and O-antigen (Fig. 3B) in the aggregates formed by the wild-type *Salmonella* strain at 6 dpi. Individual fluorescent bacteria observed in the *ssrB*-null strain were devoid of any CsgD- or CsgA-specific signals (Fig. 3A) or any O-antigen-specific signals (Fig. 3B). The amount of O-antigen detected in homogenates at 6 dpi obtained from worms infected with the *ssrB* mutant was reduced compared with wild-type infections (SI Appendix, Fig. S4). Moreover, calcofluor staining of whole intestines confirmed the presence of cellulose around colonized *Salmonella* in wild-type infections, but only a faint, nonspecific background staining was observed in infections by the *ssrB*-null strain (Fig. 3C). Specific signals for CsgD, CsgA, O-antigen, and calcofluor were absent in the *E. coli* control worms (SI Appendix, Fig. S8).

Since *E. coli* is the normal food source of worms, we examined whether the *Salmonella* aggregates in the intestines also contained *E. coli*. After exposing the L4 larvae to mCherry-expressing wild-type *Salmonella* for 1 d, we shifted the worms to a plate containing a GFP-expressing *E. coli* strain. Confocal fluorescence imaging of such live infected worms illustrated that mCherry-expressing *Salmonella* formed pure aggregates in the intestine and GFP-expressing *E. coli* were excluded from this organization (Fig. 3D).

Visualization of the ultrastructure of *Salmonella* aggregates in *C. elegans* intestines by transmission electron microscopy (TEM) is challenging, owing to the presence of intact *E. coli* in the intestinal lumen (Fig. 4A). To circumvent this problem, we fed

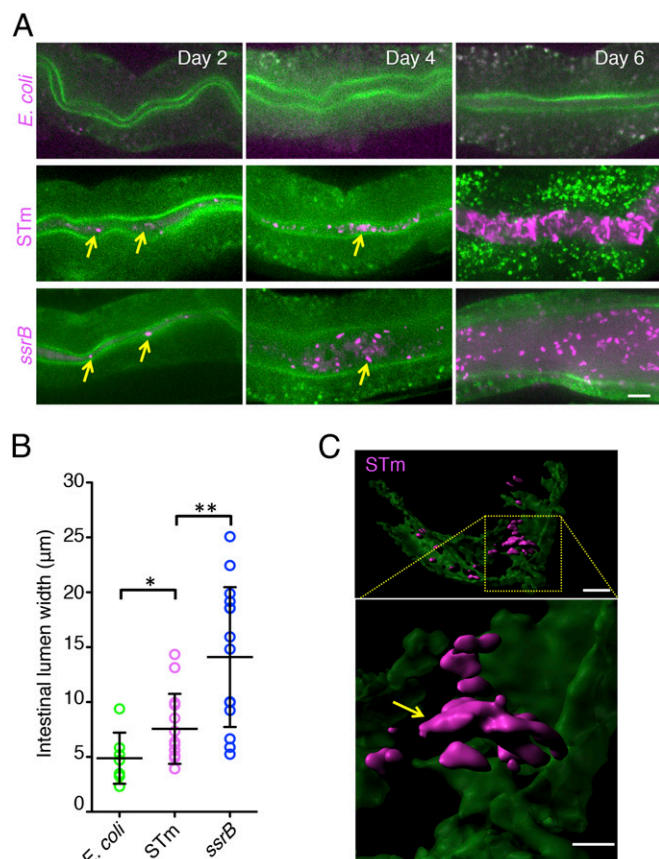


**Fig. 1.** SsrB-dependent formation of aggregates. (A) STm and *ssrB* colonized intestines (green) at 2 and 4 dpi (arrows). STm formed aggregates (magenta, Right Middle) at 6 dpi. *E. coli*-fed control worms were not colonized. (Scale bar:  $10 \mu\text{m}$ .) (B) Differences in intestinal luminal width between STm and *E. coli* and STm and *ssrB* infections at 6 dpi (mean  $\pm$  SD,  $n \geq 7$  worms). \* $P = 0.05$  and \*\* $P = 0.005$ . (C) Superresolution imaging of STm clusters (magenta) in the intestinal lumen (green) at 6 dpi. (Scale bars:  $5 \mu\text{m}$ ; Inset,  $2 \mu\text{m}$ .)

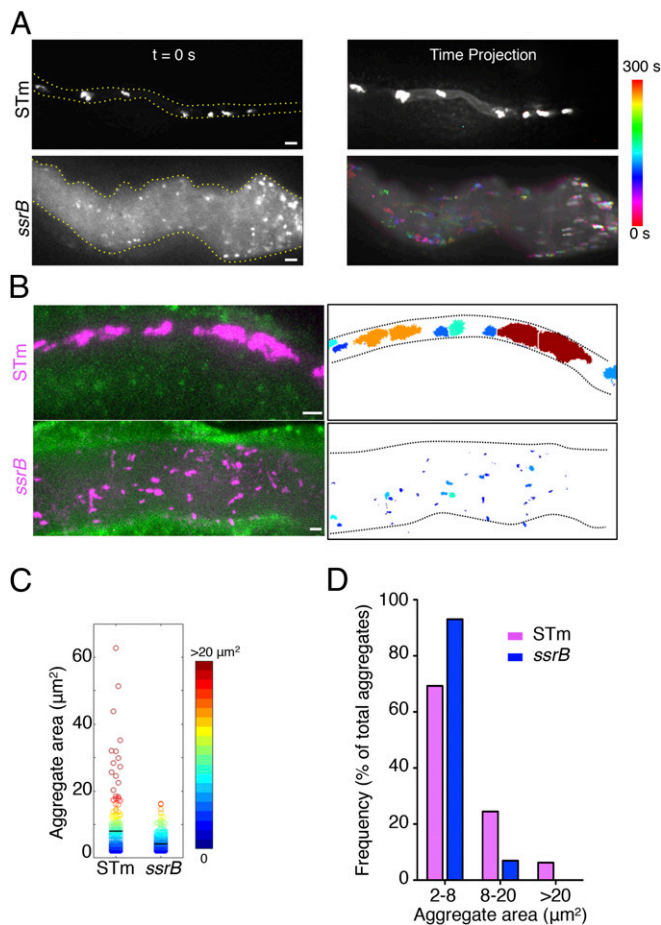


**Fig. 2.** Intestinal STm aggregates are static. (A, Left) Single confocal image ( $t = 0$  s) of worms persistently infected with STm or *ssrB* null at 6 dpi. (A, Right) Time-lapse projection of the same worms obtained at  $t = 300$  s. The mobility was determined through a series of acquisitions at 1-s intervals, and the mobility of *Salmonella* was color-coded according to the heat map on the right side. STm aggregates were completely immobile (white, Right Upper), while *ssrB*-null appeared as a range of mobilities (magenta, green blue, etc.; Right Lower) in the intestinal lumen. Dotted lines indicate intestinal boundaries. (B, Left) STm aggregates and planktonic *ssrB*-null as visualized at 6 dpi in persistently infected intestines. (B, Right) Panels are color-coded according to the heat map for area measurements in C. Large aggregates were only visible in the STm infections and were absent in the *ssrB*-null strain. (Scale bars: 10  $\mu\text{m}$ .) Measurements of the aggregate area for STm and *ssrB* infections (C) and frequency distribution of the same infections at 6 dpi (D) are shown. STm aggregates have a maximum area of 60  $\mu\text{m}^2$  ( $n \geq 12$  worms).

*E. coli* lysates to persistently infected worms before TEM analysis at 6 dpi. In persistent infections by wild-type *Salmonella*, we detected an electron-dense matrix around bacteria present in close proximity to the glycocalyx layer of the intestinal microvilli (Fig. 4A, asterisks). This dense matrix was absent in the intestinal lumen of worms persistently infected with the *ssrB*-null strain, corroborating our confocal fluorescence imaging (Fig. 3 A–C). Few bacteria and no matrix were observed in the *E. coli* control intestine (Fig. 4A).

**Planktonic *Salmonellae* Are Detrimental to Chronic Survival.** We next investigated how the ability of *Salmonella* to form biofilms affected host survival. We monitored worms after 24-h exposure to a control *E. coli*, wild-type, or *ssrB*-null *Salmonella* strain. A representative curve is shown in Fig. 4B. Both wild-type and *ssrB*-null *Salmonella* rapidly killed the worms, compared with the OP50 control. Worms persistently infected with wild-type *Salmonella*

(harboring biofilms in the intestine) lived longer (13 dpi) compared with those infected with the *ssrB*-null strain (11 dpi), which did not form biofilms (Fig. 4B). A reduction in lifespan was also observed for worms persistently infected with the biofilm double mutant *csgD csgA* strain (SI Appendix, Fig. S5). This established that the SsrB-driven lifestyle switch to form biofilms conferred *Salmonella* dormancy (i.e., a nonpathogenic carrier state), which led to an adaptive advantage in vivo. Thus, a clear causal link between formation of biofilms and dormancy is established, and the formation of biofilms in vivo prolongs colonization and survival of *Salmonella*.

**Formation of Biofilms Down-Regulates Virulence.** To investigate the molecular basis for rapid death in worms infected with the *ssrB*-null mutant, we analyzed our recent RNA-sequencing (RNA-seq) data on wild-type and *ssrB*-null strains isolated during

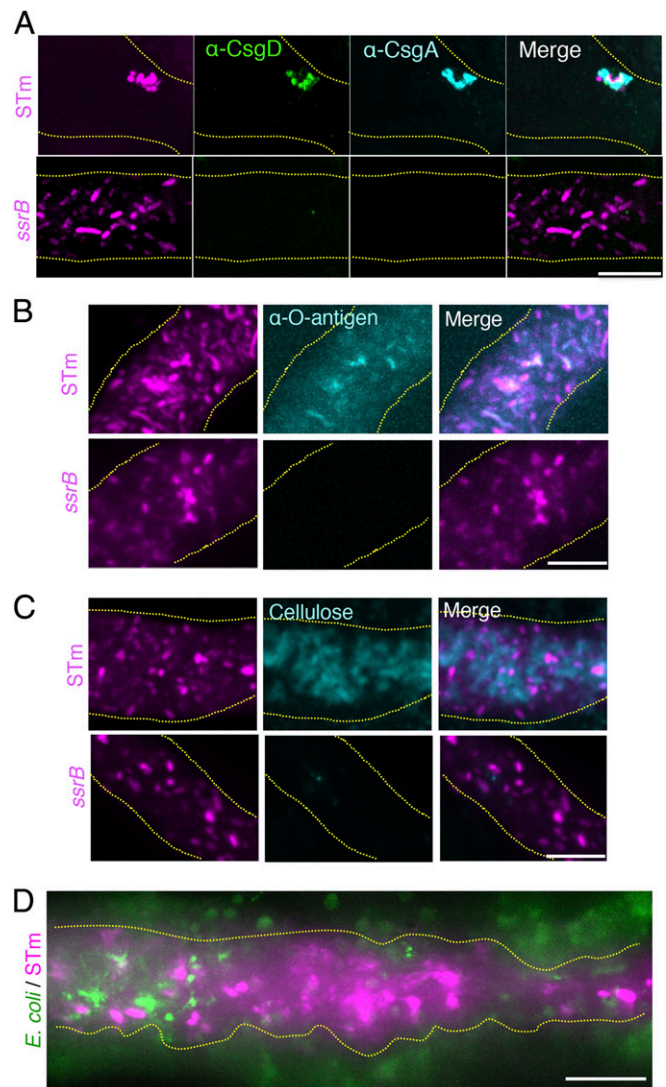


**Fig. 3.** STm aggregates express biofilm markers and exclude *E. coli*. (A and B) STm aggregates (magenta), but not *ssrB*-null, express the biofilm regulator CsgD (green), the curli subunit CsgA (cyan), and O-antigen (cyan), as detected by immunostaining of isolated intestines at 6 dpi. (C) The presence of cellulose (cyan) was detected by calcofluor staining in only the STm-infected intestines (magenta) at 6 dpi. (D) *E. coli* (green), a normal dietary component, was not a part of luminal STm aggregates (magenta) at 6 dpi. Dotted lines indicate intestinal boundaries. (Scale bars: 10  $\mu\text{m}$ .)

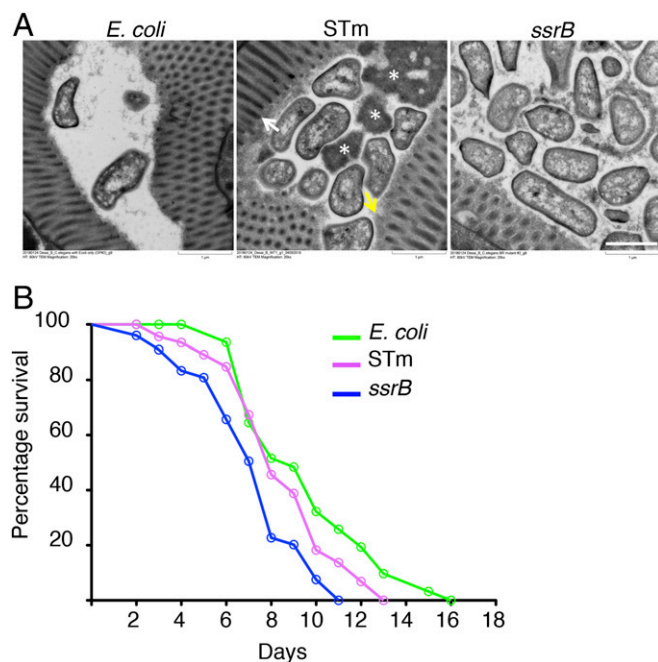


**Fig. 4.** The absence of biofilms leads to premature worm death. (A) Intestines of STm-infected worms showed the presence of an electron-dense matrix (white asterisks) around bacteria near the glycocalyx layer (yellow arrow) of the intestinal microvilli (white arrow), as observed by TEM imaging. (Scale bar: 1  $\mu\text{m}$ .) (B) Worms colonized with the biofilm mutant *ssrB*-null die faster, leading to 100% death at 11 dpi compared with 100% death at 13 dpi for STm infections. Control worms survive for 16 d ( $n = 2$ , with a total of 50 worms in each group).

growth of in vitro biofilms. SPI-1 genes, which are important for uptake by intestinal epithelia (reviewed in ref. 1) and pathogenesis in worms (23), were significantly up-regulated in the *ssrB* mutant (SI Appendix, Table S1). To validate this result, we measured the transcript levels of the SPI-1 regulator, *fliZ* (24); the SPI-1-encoded transcriptional activators, *hilD*, *hilA*, and *invF*; and the SPI-1 effector, *sptP*, in the wild-type and *ssrB*-null strains by qRT-PCR. Normalized transcript levels were increased, including: *fliZ* (~fivefold), *hilD* (~fourfold), *hilA* (~sevenfold), *invF* (~fivefold), and *sptP* (~fourfold) in the *ssrB*-null strain (Fig. 5A), consistent with our RNA-seq results. We next performed qRT-PCR analysis of SPI-1 transcripts from worms persistently infected with wild-type and *ssrB*-null strains of *Salmonella*. At 6 dpi, there was an up-regulation of in vivo transcript levels of *fliZ* (~12-fold), *hilD* (~10-fold), and *sptP* (~sevenfold) in the *ssrB*-null background (Fig. 5B). Thus, in persistent infections of wild-type *Salmonella*, SsrB drove biofilm formation (Figs. 1–3) and inhibited the expression of virulence genes encoded by SPI-1 (Fig. 5D and Discussion).

**Biofilms Promote Innate Immunity.** The SPI-1 effector SptP is known to disrupt *Salmonella*-induced mitogen-activated protein kinase (MAPK) signaling by decreasing the levels of active phospho-extracellular signal-regulated kinase (ERK) [mitogen-activated protein kinase kinase (MAPKK)] (25), thereby targeting a conserved p38/MAPK innate immunity pathway in *C. elegans* (23). Since SptP was up-regulated in the *ssrB*-null infection (Fig. 5A and B), we hypothesized that the premature worm death (Fig. 4B) was due to a decrease in p38/MAPK innate immunity (23). To test this hypothesis, we probed the levels of phospho-SEK-1 (ERK homolog) in worms persistently infected with wild-type and *ssrB*-null *Salmonella* strains at 6 dpi by Western blotting. Antibodies against total SEK-1 and tubulin served as controls. We observed that phospho-SEK-1 was undetectable in

*ssrB*-null infections, in contrast to the wild type (Fig. 5C). Thus, SptP levels were inhibited by SsrB in the in vivo biofilms formed by wild-type *Salmonella*, and this led to activation of p38/MAPK innate immunity signaling (Fig. 5D and E). In the absence of SsrB, when biofilms are absent in the worm gut, SptP disrupts host innate immunity by decreasing the levels of phospho-SEK-1 (Fig. 5C).

Finally, when worms were persistently infected with an *ssrB sptP* double mutant, intestinal aggregates were not formed at 6 dpi (SI Appendix, Fig. S6) and the premature death was rescued. The worms survived similar to wild-type infections (SI Appendix, Fig. S7). In the absence of *sptP* alone, in vivo aggregates were formed in persistent infections (SI Appendix, Fig. S6), activation of the p38/MAPK innate immunity pathway was intact, and the time to death was similar to the wild type (SI Appendix, Fig. S7).

## Discussion

Herein, we unraveled the basis of dormancy in persistent infections by investigating *Salmonella* biofilms during infection of a live heterologous host, *C. elegans*. These findings are significant, because *Salmonella* is known to form biofilms in chronically infected humans (26, 27). Colonization of *Salmonella* Typhimurium in host tissues such as chicken intestinal epithelia and human epithelia also required the formation of multicellular biofilms (28), although the regulatory mechanisms remained unknown. In the present work, we established that pathways established for in vitro biofilm formation (5) were also important in vivo. However, understanding the adaptive advantage conferred by a community lifestyle has remained elusive in studies using the standard mouse model of infection (6). Using persistently infected worms as model hosts, we determined that biofilms are immunoprotective and that the planktonic lifestyle was detrimental to the long-term survival of *Salmonella* in vivo. This persistent lifestyle involves both cross-talk between two major pathogenicity islands in *Salmonella* (SPI-1 and SPI-2) and up-regulation of the biofilm pathway by the central regulator SsrB. Our present studies thus unravel the significance of SsrB-driven biofilms for enabling in vivo dormancy, which leads to prolonged carriage in asymptomatic hosts.

Static aggregates of *Salmonella* were visible in persistently infected intestines (Figs. 1A and 2A and Movie S2) that ranged in size from 10 to 60  $\mu\text{m}^2$  (Fig. 2C) and were encased in an extracellular matrix composed of curli, cellulose, and O-antigen, typical of *Salmonella* biofilms (Fig. 3A–C). Superresolution microscopy validated their presence in the intestinal lumen and provided high-resolution visualization of *Salmonella* dormancy in vivo (Fig. 1C and Movie S1). Further, TEM enabled finer observation of matrix-encased aggregates near the glycocalyx layer of the intestinal microvilli in worms infected with wild-type *Salmonella*. It remains to be determined whether infection by wild-type *Salmonella* prevents motility in the intestinal lumen or is a direct result of aggregate formation. In the future, it will be worthwhile to determine the exact components of the glycocalyx layer and the surrounding epithelial tissue that are exploited by bacterial pathogens to survive as matrix-encased aggregates in vivo. An aggregative lifestyle has also been implicated in chronic infections of *Pseudomonas aeruginosa* in the cystic fibrosis lung (29), in a hyperinfectious lifestyle in *V. cholerae* (8), and as matrix-encased three-dimensional structures in *Vibrio* biofilms in vitro (30). Commensal *E. coli* was excluded from the intestinal aggregates of *Salmonella* (Fig. 3D) via an as yet unknown mechanism that could be mediated by the *Salmonella* type VI secretion system (31, 32). Importantly, bacteria were present throughout the *C. elegans* gut (Fig. 3D), indicating that the grinder was not sufficient for bacterial elimination (16). The *C. elegans* persistent infection model can now be harnessed to visualize the formation of mixed species biofilms in hosts and further understand the mechanisms that enable cooperation or competition between colonizing gut bacteria.



**Lifespan Analysis.** For survival analysis, 50 to 60 N2 worms were placed on OP50 *E. coli* plates postinfection and counted daily. Worms that failed to respond to probing by eyelash touch were considered dead. Worms that died due to drying up on the walls of the plates were excluded from survival analyses. The experiment was done twice to include biological replicates. All calculations were carried out in Excel and plotted using GraphPad Prism 6 Software.

**Immunofluorescence and Live Imaging.** For live imaging, worms were mounted with 0.2 mM levamisole on a 3% agarose pad on a glass slide, closed with a coverslip, and sealed with wax. Immunofluorescence of in vivo STm aggregates was conducted on surgically extruded intestine according to a method by Barth Grant (<https://wormatlas.org/gonadintest.htm>). Briefly, worms at 6 dpi were collected and washed in egg buffer and immobilized in 0.2 mM levamisole. The immobilized worms were decapitated using hypodermic needles, allowing the intestine to extrude. Intestines were then fixed using 1.25% paraformaldehyde in egg buffer. Subsequently, the fixed samples were placed in 1× PBST-bovine serum albumin (PTB; 1%) for 1 h at RT. This was followed by a 45-min incubation in PTB containing 100 μg/mL lysozyme and 5 mM ethylenediaminetetraacetic acid. The intestine samples were then incubated overnight at 4 °C in primary antibodies against CsgD (1:3 dilution, anti-mouse; a kind gift from Aaron White, University of Saskatchewan, Saskatoon, SK, Canada), CsgA (1:1,000 dilution, anti-rabbit; a kind gift from Matthew Chapman, University of Michigan, Ann Arbor, MI), and O-antigen (1:1,000 dilution, anti-rabbit; a kind gift from Aaron White). Subsequently, the samples were stained at RT using anti-mouse secondary antibodies Alexa Fluor 488 (1:1,000 dilution) and anti-rabbit Alexa Fluor 405 (1:1,000 dilution) (Life Technologies, Singapore). Imaging was done three times with at least 10 worms in each infection set.

**RNA Isolation from Persistently Infected Worms.** Around 100 worms were collected at 6 dpi washing two to three times in 1× PBST and stored at –80 °C or used immediately for RNA isolation. Total RNA isolation and DNase treatment were done as described above. DNase-treated samples were then depleted of host RNA using the MICROBEnrich Kit (Thermo Fisher Scientific, Singapore). This was followed by enrichment of bacterial mRNA using the MICROExpress Kit (Thermo Fisher Scientific, Singapore).

**ACKNOWLEDGMENTS.** We thank our colleagues at the Mechanobiology Institute for the following: Danesha Suresh and Jason Lim from the R.Z.-B. laboratory for assistance with worm maintenance, Ong Hui Ting for help with image analysis, Ti Weng for providing anti-phospho-SEK-1 and anti-total SEK-1 antibodies, and Diego Piita de Araujo and Melanie Lee for scientific illustrations. We thank Alexander Westermann and Jörg Vogel (Institute for Molecular Infection Biology), for helping to troubleshoot RNA isolations from persistently infected worms. We are grateful to Michael Sheetz (Mechanobiology Institute), Stephen Lory (Harvard Medical School), and Lalita Ramakrishnan (University of Cambridge) for comments on the manuscript. We acknowledge the CGC, which is funded by the NIH Office of Research Infrastructure Programs (Grant P40 OD010440), for providing strain S5104. We thank Matt Chapman (University of Michigan) for the kind gift of anti-CsgA antibody and Aaron White (University of Saskatchewan) for anti-CsgD and anti-O-antigen antibodies. We acknowledge the A\*STAR Microscopy Platform/Electron Microscopy for assistance in sample processing and TEM imaging in this study and David Liebl, Head of Electron Microscopy, for additional comments. This study was funded by Research Centre of Excellence in Mechanobiology, National University of Singapore, Ministry of Education, Singapore and Grants MOE2018-T2-1-038, NIHR21-A1123640, and VA 510 1 BX000372 (to L.J.K.).

1. J. R. Ellermeier, J. M. Schlauch, Adaptation to the host environment: Regulation of the SPI1 type III secretion system in *Salmonella enterica* serovar typhimurium. *Curr. Opin. Microbiol.* **10**, 24–29 (2007).
2. A. K. Lee, C. S. Detweiler, S. Falkow, OmpR regulates the two-component system SsrA-SsrB in *Salmonella* pathogenicity island 2. *J. Bacteriol.* **182**, 771–781 (2000).
3. X. Feng, R. Oropeza, L. J. Kenney, Dual regulation by phospho-OmpR of *ssrA/B* gene expression in *Salmonella* pathogenicity island 2. *Mol. Microbiol.* **48**, 1131–1143 (2003).
4. X. Feng, D. Walthers, R. Oropeza, L. J. Kenney, The response regulator SsrB activates transcription and binds to a region overlapping OmpR binding sites at *Salmonella* pathogenicity island 2. *Mol. Microbiol.* **54**, 823–835 (2004).
5. S. K. Desai *et al.*, The horizontally-acquired response regulator SsrB drives a *Salmonella* lifestyle switch by relieving biofilm silencing. *eLife* **5**, e10747 (2016).
6. R. W. Crawford *et al.*, Gallstones play a significant role in *Salmonella* spp. gallbladder colonization and carriage. *Proc. Natl. Acad. Sci. U.S.A.* **107**, 4353–4358 (2010).
7. T. Scanu *et al.*, *Salmonella* manipulation of host signaling pathways provokes cellular transformation associated with gallbladder carcinoma. *Cell Host Microbe* **17**, 763–774 (2015).
8. S. M. Faruque *et al.*, Transmissibility of cholera: In vivo-formed biofilms and their relationship to infectivity and persistence in the environment. *Proc. Natl. Acad. Sci. U.S.A.* **103**, 6350–6355 (2006).
9. R. Tamayo, B. Patimalla, A. Camilli, Growth in a biofilm induces a hyperinfectious phenotype in *Vibrio cholerae*. *Infect. Immun.* **78**, 3560–3569 (2010).
10. D. Walthers *et al.*, The response regulator SsrB activates expression of diverse *Salmonella* pathogenicity island 2 promoters and counters silencing by the nucleoid-associated protein H-NS. *Mol. Microbiol.* **65**, 477–493 (2007).
11. D. Walthers *et al.*, *Salmonella enterica* response regulator SsrB relieves H-NS silencing by displacing H-NS bound in polymerization mode and directly activates transcription. *J. Biol. Chem.* **286**, 1895–1902 (2011).
12. S. Chakraborty, H. Mizusaki, L. J. Kenney, A FRET-based DNA biosensor tracks OmpR-dependent acidification of *Salmonella* during macrophage infection. *PLoS Biol.* **13**, e1002116 (2015).
13. A. T. F. Liew *et al.*, Single cell, super-resolution imaging reveals acid-dependent SsrB gene regulation. *eLife* **8**, e45311 (2019).
14. S. K. Desai, L. J. Kenney, To ~P or not to ~P? Non-canonical activation by two-component response regulators. *Mol. Microbiol.* **103**, 203–213 (2017).
15. H. Steenackers, K. Hermans, J. Vanderleyden, S. C. J. De Keersmaecker, *Salmonella* biofilms: An overview on occurrence, structure, regulation and eradication. *Food Res. Int.* **45**, 502–531 (2012).
16. A. Labrousse, S. Chauvet, C. Couillault, C. L. Kurz, J. J. Ewbank, *Caenorhabditis elegans* is a model host for *Salmonella typhimurium*. *Curr. Biol.* **10**, 1543–1545 (2000).
17. A. Aballay, P. Yorgey, F. M. Ausubel, *Salmonella typhimurium* proliferates and establishes a persistent infection in the intestine of *Caenorhabditis elegans*. *Curr. Biol.* **10**, 1539–1542 (2000).
18. J. Hodgkin, P. E. Kuwabara, B. Corneliussen, A novel bacterial pathogen, *Microbacterium nematophilum*, induces morphological change in the nematode *C. elegans*. *Curr. Biol.* **10**, 1615–1618 (2000).
19. J. W. Costerton, P. S. Stewart, E. P. Greenberg, Bacterial biofilms: A common cause of persistent infections. *Science* **284**, 1318–1322 (1999).
20. U. Römling, W. D. Sierralta, K. Eriksson, S. Normark, Multicellular and aggregative behaviour of *Salmonella typhimurium* strains is controlled by mutations in the *agfD* promoter. *Mol. Microbiol.* **28**, 249–264 (1998).
21. X. Zogaj, M. Nimtz, M. Rohde, W. Bokranz, U. Römling, The multicellular morphotypes of *Salmonella typhimurium* and *Escherichia coli* produce cellulose as the second component of the extracellular matrix. *Mol. Microbiol.* **39**, 1452–1463 (2001).
22. D. L. Gibson *et al.*, *Salmonella* produces an O-antigen capsule regulated by AgfD and important for environmental persistence. *J. Bacteriol.* **188**, 7722–7730 (2006).
23. J. L. Tenor, B. A. McCormick, F. M. Ausubel, A. Aballay, *Caenorhabditis elegans*-based screen identifies *Salmonella* virulence factors required for conserved host-pathogen interactions. *Curr. Biol.* **14**, 1018–1024 (2004).
24. J. E. Chubiz, Y. A. Golubeva, D. Lin, L. D. Miller, J. M. Schlauch, Fliz regulates expression of the *Salmonella* pathogenicity island 1 invasion locus by controlling HilD protein activity in *Salmonella enterica* serovar typhimurium. *J. Bacteriol.* **192**, 6261–6270 (2010).
25. S. Murli, R. O. Watson, J. E. Galán, Role of tyrosine kinases and the tyrosine phosphatase SptP in the interaction of *Salmonella* with host cells. *Cell. Microbiol.* **3**, 795–810 (2001).
26. B. Basnyat, S. Baker, Typhoid carriage in the gallbladder. *Lancet* **386**, 1074 (2015).
27. J. S. Gunn *et al.*, *Salmonella* chronic carriage: Epidemiology, diagnosis, and gallbladder persistence. *Trends Microbiol.* **22**, 648–655 (2014).
28. N. A. Ledebauer, B. D. Jones, Exopolysaccharide sugars contribute to biofilm formation by *Salmonella enterica* serovar typhimurium on HEp-2 cells and chicken intestinal epithelium. *J. Bacteriol.* **187**, 3214–3226 (2005).
29. P. K. Singh *et al.*, Quorum-sensing signals indicate that cystic fibrosis lungs are infected with bacterial biofilms. *Nature* **407**, 762–764 (2000).
30. V. Berk *et al.*, Molecular architecture and assembly principles of *Vibrio cholerae* biofilms. *Science* **337**, 236–239 (2012).
31. T. G. Sana *et al.*, *Salmonella* Typhimurium utilizes a T6SS-mediated antibacterial weapon to establish in the host gut. *Proc. Natl. Acad. Sci. U.S.A.* **113**, E5044–E5051 (2016).
32. Y. R. Brunet *et al.*, H-NS silencing of the *Salmonella* pathogenicity island 6-encoded type VI secretion system limits *Salmonella enterica* serovar typhimurium interbacterial killing. *Infect. Immun.* **83**, 2738–2750 (2015).
33. D. M. Cirillo, R. H. Valdivia, D. M. Monack, S. Falkow, Macrophage-dependent induction of the *Salmonella* pathogenicity island 2 type III secretion system and its role in intracellular survival. *Mol. Microbiol.* **30**, 175–188 (1998).
34. D. Pérez-Morales *et al.*, The transcriptional regulator SsrB is involved in a molecular switch controlling virulence lifestyles of *Salmonella*. *PLoS Pathog.* **13**, e1006497 (2017).
35. A. L. Goodman *et al.*, A signaling network reciprocally regulates genes associated with acute infection and chronic persistence in *Pseudomonas aeruginosa*. *Dev. Cell* **7**, 745–754 (2004).
36. J. E. Irazoqui, J. M. Urbach, F. M. Ausubel, Evolution of host innate defence: Insights from *Caenorhabditis elegans* and primitive invertebrates. *Nat. Rev. Immunol.* **10**, 47–58 (2010).
37. S. Brenner, The genetics of *Caenorhabditis elegans*. *Genetics* **77**, 71–94 (1974).
38. W. Y. Ding *et al.*, Plastin increases cortical connectivity to facilitate robust polarization and timely cytokinesis. *J. Cell Biol.* **216**, 1371–1386 (2017).
39. J. E. Karlinsky, lambda-Red genetic engineering in *Salmonella enterica* serovar Typhimurium. *Methods Enzymol.* **421**, 199–209 (2007).
40. R. B. D. Davis, J. Roth, *Advanced Bacterial Genetics* (Cold Spring Harbor Laboratory Press, Cold Spring Harbor, NY, 1980), pp. 16–18.